Neutron diffraction, magnetic, and transport studies of $NdNi_4Al$

T. Toliński
Institute of Molecular Physics, Polish Academy of Sciences, M. Smoluchowskiego 17, 60-179 Poznań, Poland

W. Schäfer
Mineralogisches Institut, Univ. of Bonn, at Forschungszentrum Jülich, 52425 Jülich, Germany

W. Kockelmann
Mineralogisches Institut, Univ. of Bonn, at ISIS Facility, Rutherford Appleton Laboratory, Chilton OX11 0QX, United Kingdom

A. Kowalczyk
Institute of Molecular Physics, Polish Academy of Sciences, Smoluchowskiego 17, 60-179 Poznań, Poland

A. Hoser
Institut für Kristallographie, RWTH-Aachen, Germany

(Received 24 February 2003; revised manuscript received 5 June 2003; published 2 October 2003)

Joint investigations of the magnetic, structural, and transport properties of $NdNi_4Al$ which crystallizes in the hexagonal $CaCu_5$-type structure are reported. The transition to a ferromagnetic state at 6 K has been established from ac magnetic susceptibility and neutron diffraction measurements. The influence of external magnetic fields has been also studied. The alignment of the magnetic moments has been observed to be perpendicular to the hexagonal axis. The magnetic moment of $NdNi_4Al$ in $H=6$ T was determined to be equal to $1.52\mu_B$/f.u., which was slightly reduced in comparison with $1.68\mu_B$/f.u. for $NdNi_4B$ compounds.

DOI: 10.1103/PhysRevB.68.144403 PACS number(s): 61.12.Ld, 87.64.Bx, 71.20.Eh

I. INTRODUCTION

The RNi_4Al compounds with $R=Y$ or rare earth crystallize in the hexagonal $CaCu_5$-type structure, space group $P6/mmm$. The interest in these materials originates from the successful commercial use of the $LaNi_5$ alloys by reason of their large hydrogen absorption.[1] Applications in batteries and for hydrogen storage have been performed.[2] Magnetic, electronic, structural, and thermodynamic properties of $TbNi_{5-x}Al_x$ and $LaNi_{5-x}Al_x$ hydrogen systems have already been carefully studied.[3,4] The case of $R=$ Gd, Dy, and Er was also addressed.[5–7] Our interest in the RNi_4Al series is a consequence of our previous wide research on RNi_4B compounds.[8–10]

In this paper we present joint results on $NdNi_4Al$, including dc magnetization, ac susceptibility, neutron diffraction, and electrical resistivity measurements. The RNi_4Al system possesses advantages comparing with the B-based compounds. The substitution of B by Al opens the possibility to carry out a detailed analysis using neutron scattering and the mentioned applications of these materials make them an important object for investigations. The RNi_4B compounds, like those of the RNi_4Al series, are characterized by zero or negligible magnetism of the Ni atoms, which simplifies the interpretation of the magnetic, transport, or electronic properties of these materials.

II. EXPERIMENT

The RNi_4Al compounds were prepared by induction melting of the stoichiometric amounts of the constituent elements in a water-cooled boat, under an argon atmosphere. The ingots were inverted and remelted several times to ensure homogeneity.

Measurements of the dc magnetization and the ac susceptibility in a magnetic field up to 9 T and temperature down to 4.2 K were carried out on a MagLab2000 instrument.

Neutron diffraction has been performed (i) in a constant-wavelength technology ($\lambda=1.0957$ Å) using the powder diffractometer SV7-a at the FRJ-2 reactor in Jülich, Germany[11] and (ii) in time-of-flight technology using the diffractometer ROTAX at the spallation source ISIS in Chilton, U.K.[12] Room- and low-temperature diffraction patterns have been collected on SV7-a; additional measurements between 1.8 and 10 K have been performed on ROTAX. The sample was contained in a cylindrical vanadium can mounted on SV7-a (1) in a refrigerator cryostat and (2) in a cryomagnet with external magnetic fields up to 5 T perpendicular to the horizontal diffraction plane and on ROTAX in a He cryostat with Al tail.

The electrical measurements were carried out by a standard four-probe technique on a rectangular-shaped sample for a correct determination of the sample resistivity.

III. MAGNETIC MEASUREMENTS

Figure 1 displays the real, χ', and the imaginary, χ'', part of the ac susceptibility for $NdNi_4Al$ compounds. The transition from the paramagnetic to the ferromagnetic state is well identified at $T_C=6$ K. For comparison in our previous studies of $NdNi_4B$, T_C was established at 11.7 K.[9] The field dependence of the $NdNi_4Al$ magnetic moment is shown in the inset of Fig. 1 together with the result for $NdNi_4B$.[9] It is seen that the magnetization curves are similar with a larger

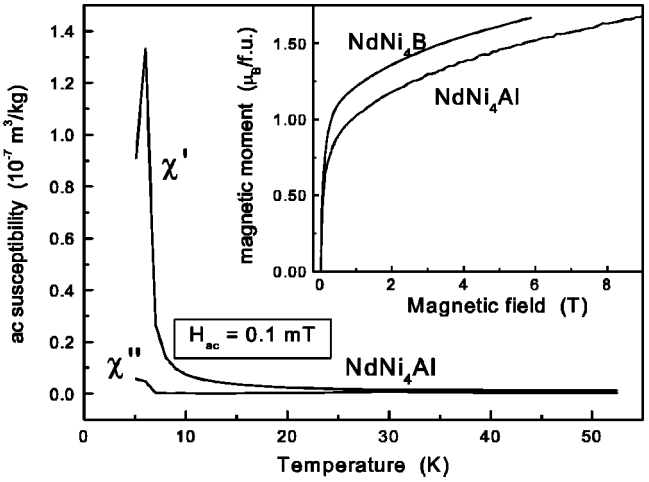

FIG. 1. The real, χ', and the imaginary, χ'', parts of the ac susceptibility for $NdNi_4Al$. Inset: the magnetization curve of the $NdNi_4Al$ and $NdNi_4B$ compounds at 4.2 K.

moment in the case of $NdNi_4B$. In an external magnetic field $H=6$ T the magnetic moment is $1.52\mu_B$/f.u. for $NdNi_4Al$ and $1.68\mu_B$/f.u. for the $NdNi_4B$ compound. It is well visible from the inset of Fig. 1 that both compounds do not saturate even in a magnetic field of 9 T. The magnetic moment of $NdNi_4Al$ is connected only with the rare earth because the Ni atoms have been claimed to be nonmagnetic in this compound. This assumption is confirmed by the present neutron diffraction studies (see next section). The nonmagnetic state of Ni has been also assumed in the case of $NdNi_4B$; however, neutron investigations of that compound are not easily accessible due to the large neutron absorption of natural boron.

IV. NEUTRON DIFFRACTION RESULTS

Figure 2 presents the neutron diffraction pattern of $NdNi_4Al$ recorded at 293 K. Full-pattern Rietveld refine-

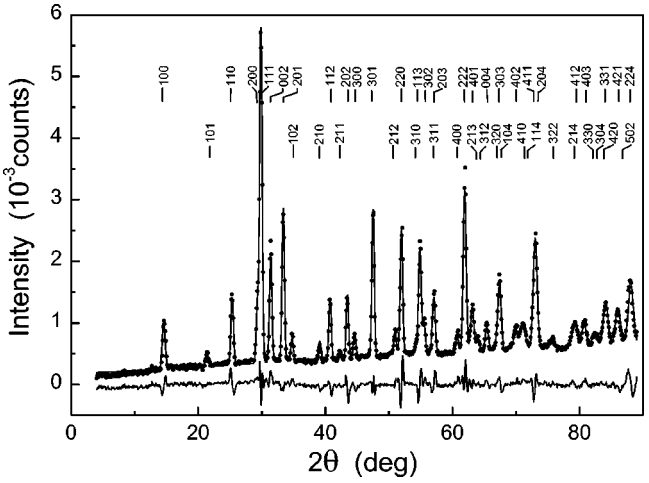

FIG. 2. Constant-wavelength neutron diffraction pattern of $NdNi_4Al$ at 293 K, experimental data (circles) and refinement (line). The bottom curve represents the difference between measurement and calculation.

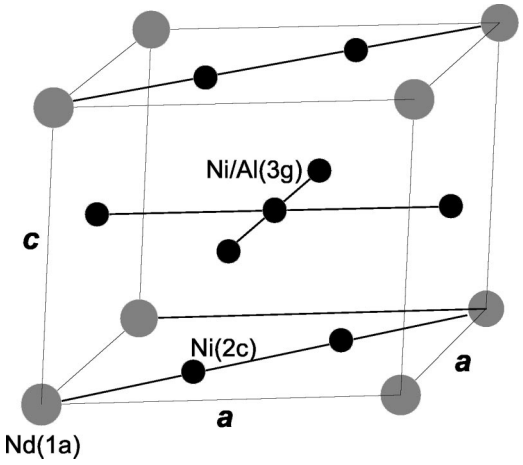

FIG. 3. Unit cell of $NdNi_4Al$.

ments using FULLPROF (Ref. 13) have been performed on the 293 K and the 4.2 K data. The refined lattice constants are $a=5.0103(13)$ Å, $c=4.0601(7)$ Å at room temperature and $a=4.9955(14)$ Å, $c=4.0551(7)$ Å at 4.2 K. The structure is described in the hexagonal space group $P6/mmm$. Nd occupies the $1a$ site (0,0,0) and Ni(1) the $2c$ site (1/3,2/3,0). Ni(2) and Al are statistically distributed on the $3g$ site (1/2,0,1/2). The Al atoms are found exclusively on the $3g$ positions and are absent on $2c$ sites, which is established owing to the fact that neutrons can well distinguish between Ni and Al due to the nuclear scattering lengths of $b=10.3$ and 3.449 fm, respectively. The unit cell is shown in Fig. 3. For comparison, the RNi_4B compounds crystallize in the structure of $CeCo_4B$ with space group $P6/mmm$. The Ni atoms occupy the crystallographic sites ($2c$) and ($6c$), the rare earth is also located in two sites ($1a$,$1b$), and boron atoms are located in the ($2d$) positions.

The 4.2 K diffraction pattern taken at SV7-a reveals neither new magnetic reflections nor intensity enhancements on nuclear reflection peak positions, at least within experimental error limits. This was the reason for additional measurements of improved peak-to-background conditions at ROTAX. A careful inspection of the temperature difference pattern

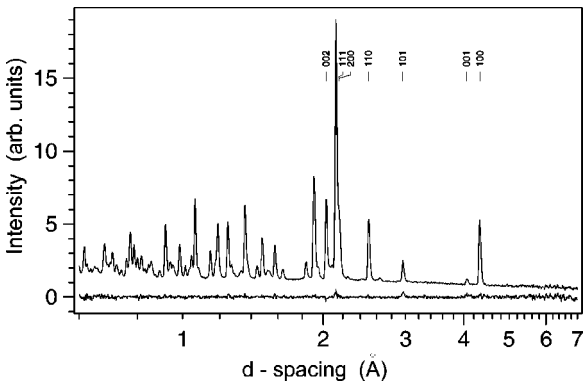

FIG. 4. Time-of-flight (d-spacing) diffraction pattern of $NdNi_4Al$ at 1.8 K and temperature difference pattern (1.8–10 K) showing the pure magnetic scattering (below); indexing of peaks with detectable magnetic scattering contributions.

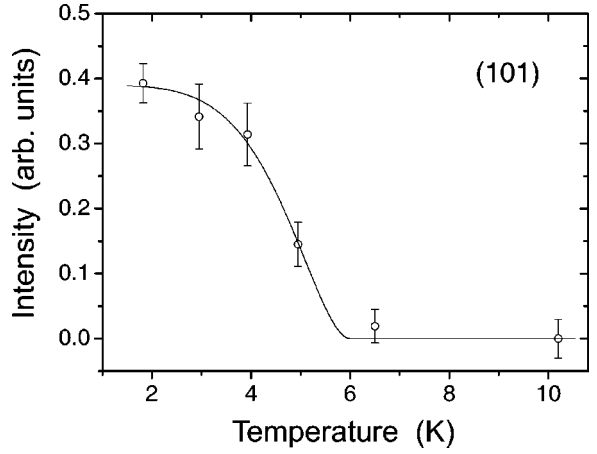

FIG. 5. Temperature dependence of the magnetic (101) reflection intensity yielding a Curie temperature of 6.0(5) K.

(1.8–10 K) reveals magnetic scattering contributions on nuclear diffraction peak positions (Fig. 4). The magnetic intensities are very weak compared to the large nuclear scattering contribution from the Ni sites. The magnetic structure has been determined by a FULLPROF refinement of the pure magnetic scattering contributions in the temperature difference pattern (range of d spacing from 2.2 to 5.0 Å). The magnetic Nd form factor has been used from Ref. 14. The magnetic intensities are in agreement with a ferromagnetic alignment of the Nd spins perpendicular to the c axis. The ordered magnetic moment amounts to $1.85(5)\mu_B$ per Nd ion at 1.8 K. The temperature dependence of the magnetic intensity confirms the Curie temperature of 6.0(5) K (Fig. 5).

The neutron diffraction experiments on SV7-a have been extended to measurements at 4.2 K in outer magnetic fields in the range from 0 to 5 T, providing a confirmation of the ferromagnetic order by additional magnetic intensities (Fig. 6). As becomes visible from the increase of the (001) and (002) and the disappearance of the (100) and (200) intensities, the ferromagnetic alignment must be perpendicular to the hexagonal axis; i.e., the moments are ordered in the hexagonal basis plane. The field dependences of the (001) and (002) reflection intensities reveal the typical magnetization curves approaching saturation with increasing field and those of (100) and (200) approaching zero. The behavior visible in Figs. 6(a) and 6(b) is in good agreement with the magnetization curve of $NdNi_4Al$ shown in the inset of Fig. 1.

The magnetic intensities are partly maintained even after switching off the external magnetic field. It is demonstrated in Fig. 7, which shows the diffraction patterns measured after changing H from value provided in the graphs to $H=0$. At temperature 4.2 K—i.e., below the ordering temperature of $NdNi_4Al$—the enlargement of some peaks—e.g., (001)—is still present after switching off the external magnetic field. At 80 K the long-range magnetic order is not visible. The behavior below 6 K is clearly a domain and hysteresis effect; i.e., it is typical of a ferromagnetic material with a small remanence.

The low transition temperature T_C and the small magnetic moment before the treatment with the magnetic field yield an important suggestion that the magnetic moment of the Ni atoms is negligible in $NdNi_4Al$. This condition simplifies the interpretation of the magnetic, transport and electronic properties of RNi_4Al or RNi_4B compounds.

V. ELECTRICAL RESISTIVITY

The phase transition observed in the magnetic experiments and discussed in previous sections is also reflected in the measurements of the temperature dependence of the electrical resistivity (see inset of Fig. 8). However, as has been observed, the jump in resistance occurs at a temperature where the absorption process (χ'') begins; this is about 20 K in the studied compound. It means that the largest changes in resistivity appear already at the stage where the irreversible losses in the system are initiated. Hence, electron scattering does not have to be most efficient at the same stage of the transition, in which the magnetic susceptibility χ'' has its maximum. Additionally, in the ac susceptibility experiment the whole volume of the sample is measured; in the case of

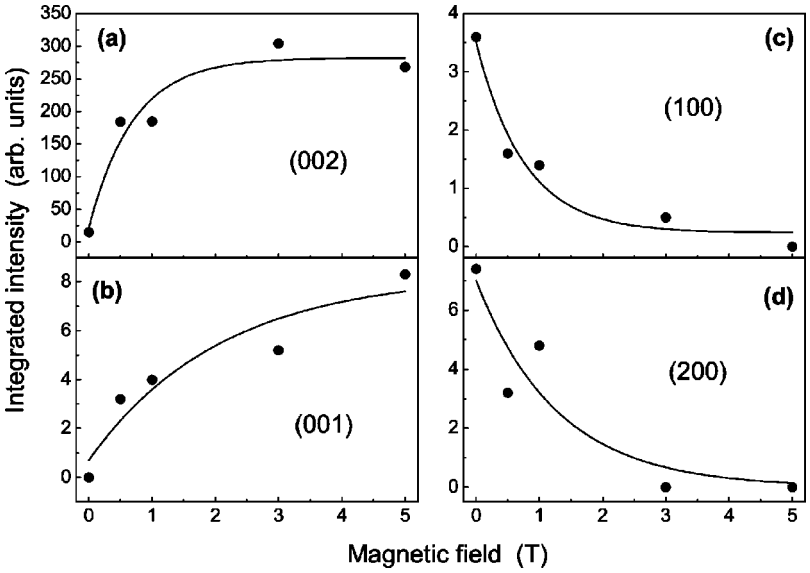

FIG. 6. The field dependence of the (001), (002), (100), and (200) reflection intensities at 4.2 K.

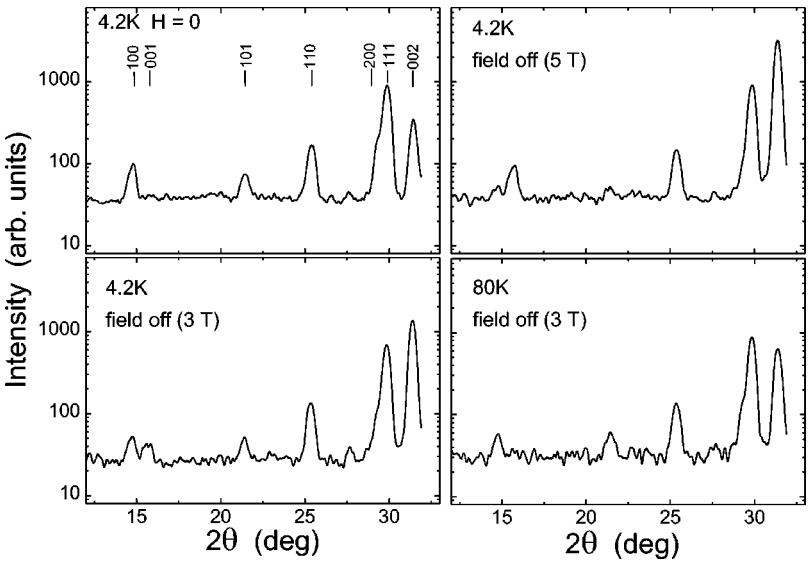

FIG. 7. Low-angle part of the neutron diffraction patterns at remanence—i.e., after switching off various external magnetic fields.

the resistance investigations mainly the contribution characterized by the highest conductivity is involved.

The $\rho(T)$ dependence of $NdNi_4Al$ illustrated in Fig. 8 consists of both the magnetic and phonon contributions. To display only the magnetic contribution within the transition area the phonon part of the isostructural nonmagnetic YNi_4Al compound was subtracted—i.e., $\rho_m(NdNi_4Al)+\rho_0 = \rho(NdNi_4Al)-\rho_{ph}(YNi_4Al)$, where $\rho(T)$ of YNi_4Al was fitted with the modified Bloch-Grüneisen relation for metallike compounds:

$$\rho(T)=\rho_0(YNi_4Al)+\rho_{ph}(T)-kT^3, \tag{1}$$

with

$$\rho_{ph}(T)=4R\Theta_D\left(\frac{T}{\Theta_D}\right)^5\int_0^{\Theta_D/T}\frac{x^5dx}{(e^x-1)(1-e^{-x})}. \tag{2}$$

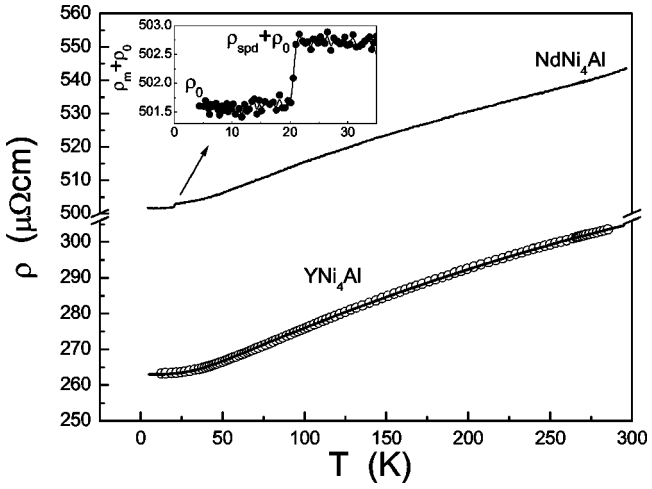

FIG. 8. Electrical resistivity of the $NdNi_4Al$ compound. The $\rho(T)$ dependence of the nonmagnetic isostructural YNi_4Al compound is also shown (bottom curve) together with a fit to formula (1). The inset shows the magnetic part $[\rho_m(NdNi_4Al)+\rho_0]$ of the $NdNi_4Al$ resistivity in the vicinity of the phase transition.

From the fit (solid line for YNi_4Al in Fig. 8) the residual resistivity is $\rho_0=263\ \mu\Omega$ cm, the constant $R=0.165\ \mu\Omega$ cm/K, the Debye temperature $\Theta_D=204$ K [for YNi_4B the Debye temperature was $\Theta_D=240$ K (Ref. 15)], and the parameter describing the scattering of the conduction electrons into a narrow d band near the Fermi level is $K=2.25\times10^{-7}\ \mu\Omega$ cm/K^3. The inset of Fig. 8 enables the estimation of the spin-disorder resistivity as $\rho_{spd}=1.14\ \mu\Omega$ cm.

Below T_C a quadratic dependence of resistivity on temperature is usually observed related to the magnon excitations, which may be modified by a presence of an energy gap. The inset of Fig. 8 shows that below T_C the resistivity ρ_m is nearly independent of temperature, implying a very large energy gap for magnons excitations in the studied $NdNi_4Al$ compound. Hence, only high-energy magnons may appear, leading to the destruction of the long-range ferromagnetic order in zero or small magnetic fields.

A large value of the residual resistivity is visible for $NdNi_4Al$. We have observed it also for other RNi_4Al compounds, while in the case of RNi_4B (Ref. 16) this value was usually below about 50 $\mu\Omega$ cm. The explanation may be based on the difference in crystallographic structures. In the case of RNi_4B the B atoms occupy the well-defined $(2d)$ sites of the $CeCo_4B$ structure, whereas the Al atoms in RNi_4Al are statistically distributed on the $(3g)$ sites of the $CaCu_5$-type structure. Therefore, the lattice disorder in the case of RNi_4Al may be responsible for the increased residual resistivity. This effect was also observed for many other compounds; e.g., the residual resistivity of RCo_2 was close to zero and after adding a small amount of Si increased up to 200 $\mu\Omega$ cm due to the appearance of a lattice disorder.[17]

VI. CONCLUSIONS

The present magnetic, neutron diffraction, and electrical resistivity studies reveal the following.

(i) The $NdNi_4Al$ compound undergoes a paramagnetic to ferromagnetic phase transition at $T_C=6$ K, as is established

both by ac susceptibility and neutron diffraction measurements. In the ferromagnetic phase the magnetic moments are ordered in the hexagonal basis plane. The magnetization curve of $NdNi_4Al$ resembles that of $NdNi_4B$, but exhibits a smaller value of the magnetic moment, which is equal to $1.52\mu_B$/f.u. for $NdNi_4Al$ and $1.68\mu_B$/f.u. for $NdNi_4B$ compounds in $H=6$ T and $T=4.2$ K. Neutron diffraction at 1.8 K provides $1.85\mu_B$ per Nd ion.

(ii) The neutron diffraction experiments support the assumption from earlier studies that the Ni atoms do not provide a ferromagnetic contribution.

(iii) The phase transition observed in the magnetic experiments is also visible in the measurements of the temperature dependence of electrical resistivity but the largest changes in resistivity appear at a temperature for which the irreversibility in the system begins. Below T_C the resistivity ρ_m is nearly independent of temperature.

ACKNOWLEDGMENTS

We are indebted to Dr. V. Ivanov for precise measurements of the electrical resistivity. This work was supported by the Center of Excellence for Magnetic and Molecular Materials for Future Electronics within the European Commission, Contract No. G5MA-CT-2002-04049. Financial support by the BMBF, Germany, under Project Nos. 03KIE8BN (SV7-a) and 03KLE8BN (ROTAX) is gratefully acknowledged.

[1] E.L. Houston and G.D. Sandrock, J. Less-Common Met. **74**, 435 (1980).
[2] M. Wada, Sci. Technol. Jpn. **51**, 54 (1994).
[3] Ž. Blažina, B. Šorgić, and A. Drašner, J. Phys.: Condens. Matter **9**, 3099 (1997).
[4] E. Burzo, S.G. Chiuzbăian, M. Neumann, and L. Chioncel, J. Phys.: Condens. Matter **14**, 8057 (2002).
[5] B. Šorgić, A. Drašner, and Ž. Blažina, J. Alloys Compd. **221**, 169 (1995).
[6] B. Šorgić, A. Drašner, and Ž. Blažina, J. Phys.: Condens. Matter **7**, 7209 (1995).
[7] B. Šorgić, A. Drašner, and Ž. Blažina, J. Alloys Compd. **232**, 79 (1996).
[8] T. Toliński, G. Chełkowska, and A. Kowalczyk, Solid State Commun. **122**, 145 (2002).
[9] T. Toliński, A. Kowalczyk, A. Szlaferek, M. Timko, and J. Kováč, Solid State Commun. **122**, 363 (2002).
[10] T. Toliński, A. Kowalczyk, and G. Chełkowska, Phys. Lett. A **308**, 75 (2003).
[11] W. Schäfer, E. Jansen, R. Skowronek, and A. Kirfel, Physica B **234-236**, 1146 (1997).
[12] W. Kockelmann, M. Weisser, H. Heinen, A. Kirfel, and W. Schäfer, Mater. Sci. Forum **321-324**, 332 (2000).
[13] J. Rodriguez-Carvajal, Physica B **192**, 55 (1999).
[14] P.J. Brown, in *International Tables for Crystallography*, edited by A.J.C. Wilson (Kluwer Academic, Dordrecht, 1995), Vol. C, p. 391.
[15] T. Toliński, A. Kowalczyk, M. Pugaczowa-Michalska, and G. Chełkowska, J. Phys.: Condens. Matter **15**, 1 (2003).
[16] T. Toliński, A. Kowalczyk, and V. Ivanov, Phys. Status Solidi B (to be published).
[17] A. Kowalczyk, J. Baszyński, J. Kováč, and A. Szlaferek, Magn. Magn. Mater **176**, 241 (1997).